# Effect of Functional and Electron Correlation on the Structure and Spectroscopy of the $Al_2O_3(001)$-$H_2O$ Interface: Supplemental Information

Mark J. DelloStritto,[†,‡] Stephan M. Piontek,[†,‡] Michael L. Klein,[†,¶,‡] and Eric Borguet[*,†,‡]

†*Department of Chemistry*

‡*Center for Complex Materials from First Principles*

¶*Institute for Computational Molecular Science, Temple University, Philadelphia, Pennsylvania 19122, United States*

E-mail: eborguet@temple.edu

## Radial Distribution Function

In Figure S1 we plot the O-O radial distribution function (RDF) for the O atoms which are part of $H_2O$ molecules in our DFT-MD simulations of the $Al_2O_3$(001)-$H_2O$ interface. Note that the water becomes less structured as we go from PBE to PBE-TS to SCAN. RPBE is actually understructured compared to all other functionals, possibly due to a slight compression of the water between the interfaces because of the unrealistically large distance of the first water layer from the oxide surface.

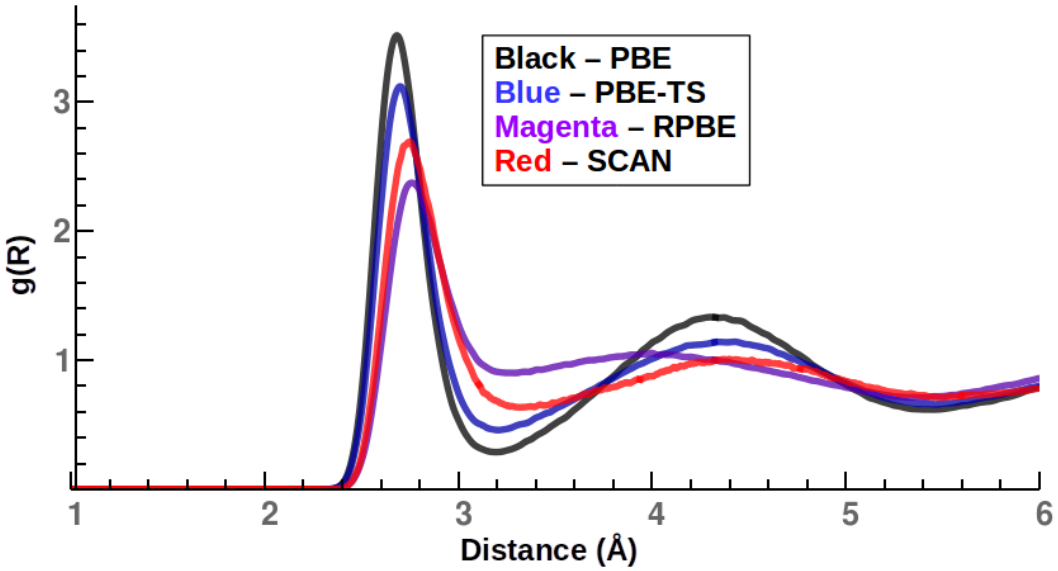


Figure S1: The O-O RDF for the O atoms which are in $H_2O$ molecules.

## SFG Spectrum - Component Decomposition

The SFG spectrum for the $Al_2O_3$(001)-$H_2O$ interface generated from the SCAN trajectories was decomposed into contributions from the $H_2O$ molecules and the surface aluminols (Figure S2). Note that the SFG spectrum can be written as the Fourier transform of a correlation function between the time derivatives of the polarizability and dipole moment of a system:

$$\chi^{(2)} = (i\omega kT)^{-1}\mathscr{F}[\langle\dot{\alpha}(t)\dot{\mu}(0)\rangle] \quad (1)$$

where $\dot{\alpha}$ and $\dot{\mu}$ are the time derivatives of the polarizability and dipole moment of the entire system. Since we can write each of these as sums over atom or bond polarizabilities and dipole moments,[1,2] we can choose to sum only over certain atoms or bonds of interest in the simulation. We can therefore decompose the spectrum by including either only the $H_2O$ molecules or only the surface aluminols in the sum over the polarizabilities and dipole moments. Note that we calculate effective polarizabilities of all bonds in the system using a Thole-type model[1,2] and we calculate self-consistent dipole moments for each bond, starting from nominal atomic charges taken from the ClayFF force field.[3] Finally, note that when calculating the polarizabilities and dipole moments all interactions are taken into account. It is only after the polarizabilities and dipole moments are generated from the trajectories that we sum over a subset of the system. The calculations reveal that the $\sim$3200 $cm^{-1}$ peak is contributed almost entirely from $H_2O$ molecules while the $\sim$3400 $cm^{-1}$ has a strong contribution from the surface aluminols Figure S2. That is not to say that the $H_2O$ molecules do not contribute any intensity to the 3400 $cm^{-1}$ peak, rather we emphasize that the contribution of the aluminols is essential for an accurate SFG spectrum with the correct relative intensity of the 3200 $cm^{-1}$ and 3400 $cm^{-1}$ peaks.

## SFG Spectrum - Depth Dependence

It is clear from Figure 2 in the main manuscript that the SFG spectrum strongly depends on the choice of functional and the accuracy of the spectrum depends on the resolution of the chosen experimental reference. SCAN significantly narrows the width of the spectrum, matching the width of the high-resolution experimental spectrum while avoiding the erroneous blue-shift associated with RPBE. To better understand the differences between the spectra obtained using different functionals, we investigate the depth dependence of the SFG spectra by altering the number of $H_2O$ molecules we include in the SFG calculation.[4] We do so by including $H_2O$ molecules within the first 5, 10, and 15 Å of the interface and plotting

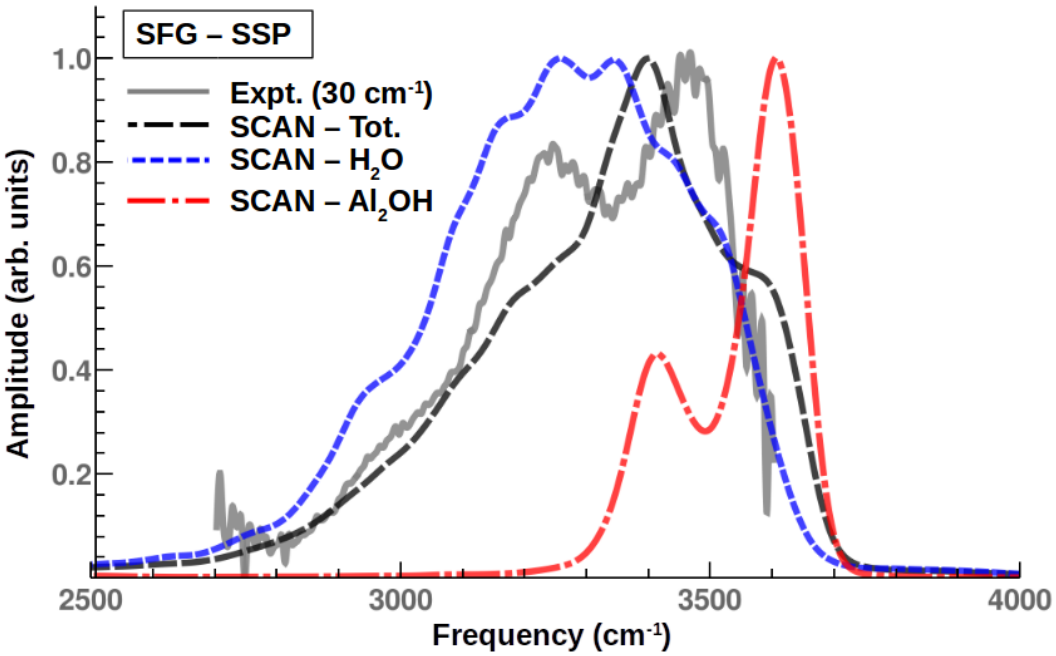


Figure S2: The SFG spectrum calculated from trajectories generated using the SCAN functional. The gray solid line depicts the experimental spectrum for a resolution of 30 $cm^{-1}$. The dashed, dotted, and dashed-dotted lines depict the SFG spectra calculated from all bonds in each half of the unit cell, only the bonds in $H_2O$ molecules, and only the bonds in aluminols, respectively.

the resulting spectra for the PBE and SCAN functionals in Figure S3. Similar calculations of a neutral quartz-water interface[5] indicate that the SFG spectrum should converge within roughly 9 Å. This is not strictly true for either functional our simulations, however, the changes beyond 10 Å are very small. Thus, we believe this discrepancy in depth dependence is a consequence of the small cells and short times of DFT-MD, as there is a decrease in the depth dependence when going from more structured water (PBE) to less structured water (SCAN), even with shorter simulations. Thus, with longer times or larger cells, we believe the depth dependence will be reduced further and the SCAN SFG spectrum will converge closely to the experimental spectrum.

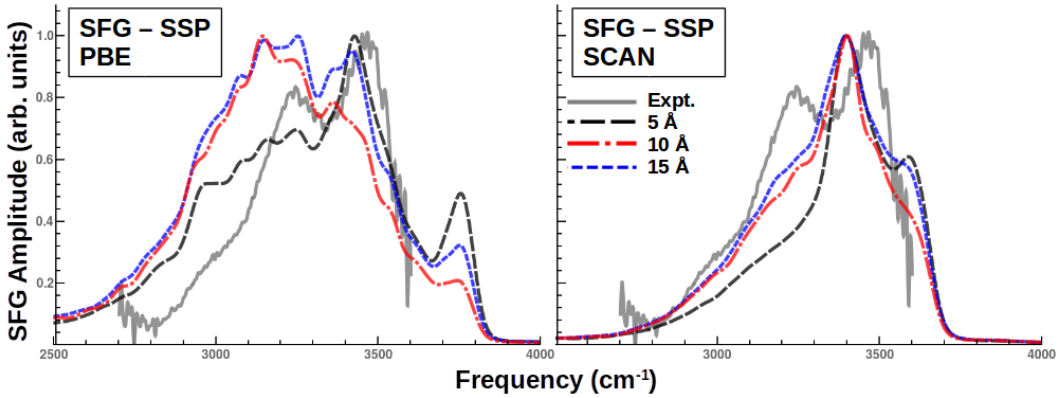


Figure S3: The depth dependence for the SFG spectra of the $Al_2O_3$(001)-$H_2O$ interface for SSP polarization for the PBE and SCAN functionals. The black, blue, and red lines for each plot depict the SFG spectrum when including the $H_2O$ molecules within the first 5, 10, and 15 Å of the alumina surface, respectively.

# Polarizability Parameters

As mentioned above, we use a Thole-type model to calculate the polarizability for all the bonds in the system. This model includes short-range corrected dipole interactions to calculate effective, additive atomic polarizabilities from initial gas-phase atomic polarizabilities. The parameters for this model are a distance scaling parameter a and the gas-phase polarizabilities for each element in the system. We fit these parameters to DFT polarizabilities of the $H_2O$ molecule for 576 configurations and the ground state configuration for the $Al(OH)_3$

molecule. We calculate the polarizabilities of the molecules using the $\omega$B97XD[6] functional and the dAug-cc-pVTZ[7,8] basis set as implemented in Gaussian16.[9] The parameters for the Thole model are presented in Table 1.

**Table 1: Parameters for Thole Polarizability Model**

| Parameter | Value |
|---|---|
| a | 1.96069 |
| $\alpha_H^{(0)}$ | 0.34 Å$^3$ |
| $\alpha_O^{(0)}$ | 1.40 Å$^3$ |
| $\alpha_{Al}^{(0)}$ | 1.65 Å$^3$ |

We present the results of the fit for the $H_2O$ molecules in Figure S4, comparing the Thole polarizabilities to the ab-initio polarizabilities. We see that, while the Thole model underestimates the magnitude of the change of the polarizability with changes in the O-H bond distance, it does reproduce the qualitative dependence of the polarizability on the molecular coordinates. Since we are concerned primarily with the relative magnitudes of the polarizabilities of the O-H bonds in the system and their frequency dependence in the O-H stretching region, we are confident in using this model to calculate the SFG spectrum of the $Al_2O_3$(001)-$H_2O$ interface.

# Sample Preparation Experimental details

We use $\alpha$-$Al_2O_3$(0001) cut equilateral roof prisms (15 x 13 x 13 x 15 mm) are the alumina surfaces for our experiments. The 15 x 15 mm$^2$ surface (opposite of roof) was the sampling area. Prisms were first cleaned with "piranha" solution (1 vol conc. $H_2O_2$: 3 vol conc. $H_2SO_4$) for $\sim$30 min in a Teflon container. *CAUTION: Piranha solution is extremely dangerous and should be handled with proper personal protective equipment.* To remove any remaining piranha solution prisms are rinsed with copious amounts of deionized water (>18.2 M$\Omega$ cm resistivity, Thermoscientific Barnstead Easypure II purification system with UV lamp) and dried using ultra high purity $N_2$ gas. The sample holder, Teflon o-ring, and prism were then

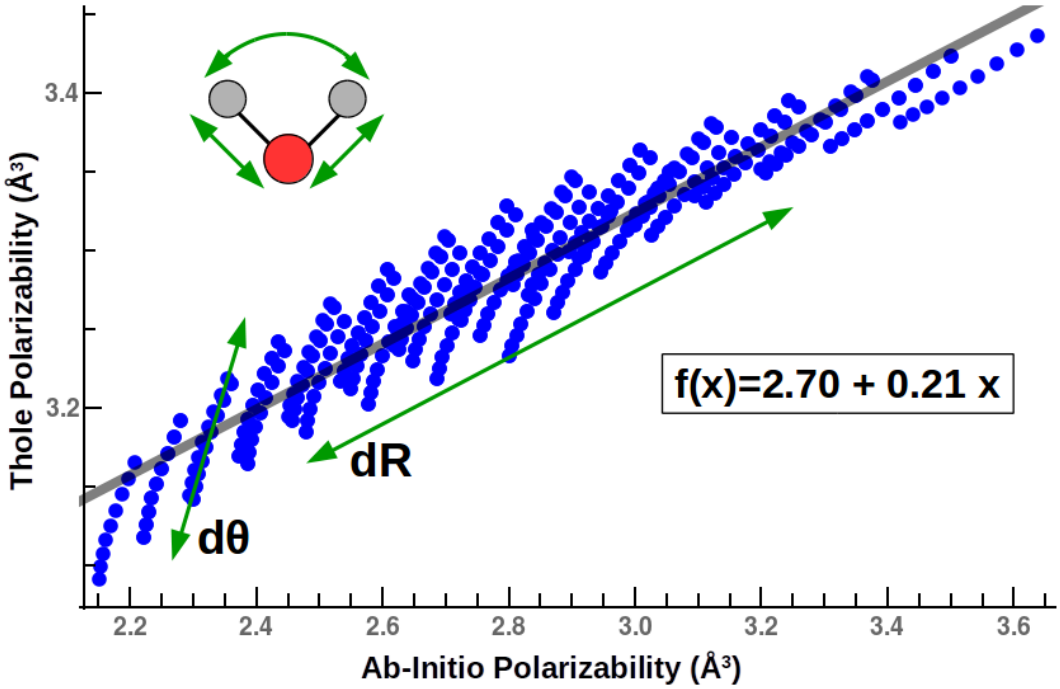


Figure S4: Plot of the ab-initio vs. Thole polarizability of a $H_2O$ molecule for 576 different configurations obtained by varying the H-O-H angle and two O-H bonds. The line is a linear fit to the data, with the function shown in the plot.

exposed to low RF plasma for 30 minutes to remove any organic contaminants. All items in the plasma cleaner equilibrate to room temperature under vacuum followed by direct assembly of the sample apparatus. A second prism coated with ∼100 nm of Au is used as a nonresonant reference to characterize IR pulse profiles.

## SFG: Optical Setup

A Ti:Sapphire regenerative amplifier laser system (Coherent, LIBRA-F-1K-110-HE+) operating at 1 kHz generating 5 mJ pulses at 800 nm with a pulse duration of 120 fs. Approximately 90% of the LIBRA output pumps our commercial OPA (Coherent, TOPAS-Prime HE), leaving ∼0.5 mJ for the visible beam line. A difference frequency generation (DFG) $AgGaS_2$ crystal attached to the output of the TOPAS generates tunable pulses in the mid IR (4000 - 1600 $cm^{-1}$). We acquire vSFG spectra using a broadband IR pulse profile with

$\sim$1000 cm$^{-1}$ of bandwidth and $\sim$10 $\mu$J/pulse centered 3400 cm$^{-1}$, allowing us to probe all oscillators in the OH stretch region without spectral stitching. The 0.5 mJ of visible light (800 nm) is passed through a narrow bandpass filter resulting in $\sim$2 nm of bandwidth of $\sim$30 cm$^{-1}$. Incident angles were 60$^{\circ}$(IR 2.5 $\mu$J/pulse) and 54$^{\circ}$(Vis $\sim$30 $\mu$J/pulse) with focused beam waists of $\sim$75 and 200 $\mu$m. Reflected visible photons were removed from detection using a 750 nm shortpass filter (Melles Griot). A CCD detector (Princeton Instruments) with a spectrograph (300i Acton Research Corp.) collect the vSFG signal. vSFG spectra were normalized via division of nonresonant vSFG signal generated by a gold coated $\alpha$-$Al_2O_3$(0001) prism to characterize the IR pulse profile followed by a second division of wavelength dependent Fresnel Factor curves due to absorption of mid-IR photons from the water/alumina interface.[10]

# References


(1) Thole, B. Molecular polarizabilities calculated with a modified dipole interaction. *Chemical Physics* **1981**, *59*, 341–350.

(2) DelloStritto, M.; Sofo, J. Bond Polarizability Model for Sum Frequency Generation at the $Al_2O_3$(0001)-$H_2O$ Interface. *The Journal of Physical Chemistry A* **2017**, *121*, 3045–3055.

(3) Cygan, R. T.; Liang, J.-J.; Kalinichev, A. G. Molecular Models of Hydroxide, Oxyhydroxide, and Clay Phases and the Development of a General Force Field. *The Journal of Physical Chemistry B* **2004**, *108*, 1255–1266.

(4) Khatib, R.; Backus, E. H. G.; Bonn, M.; Perez-Haro, M.-J.; Gaigeot, M.-P.; Sulpizi, M. Water orientation and hydrogen-bond structure at the fluorite/water interface. *Scientific Reports* **2016**, *6*, 24287.

(5) Joutsuka, T.; Hirano, T.; Sprik, M.; Morita, A. Effects of third-order susceptibility in sum frequency generation spectra: a molecular dynamics study in liquid water. *Physical Chemistry Chemical Physics* **2017**,

(6) Chai, J.-D.; Head-Gordon, M. Long-range corrected hybrid density functionals with damped atomatom dispersion corrections. *Physical Chemistry Chemical Physics* **2008**, *10*, 6615–6620.

(7) Kendall, R. A.; Jr, T. H. D.; Harrison, R. J. Electron affinities of the firstrow atoms revisited. Systematic basis sets and wave functions. *The Journal of Chemical Physics* **1992**, *96*, 6796–6806.

(8) Jr, T. H. D. Gaussian basis sets for use in correlated molecular calculations. I. The atoms boron through neon and hydrogen. *The Journal of Chemical Physics* **1989**, *90*, 1007–1023.

(9) Frisch, M. J.; Trucks, G. W.; Schlegel, H. B.; Scuseria, G. E.; Robb, M. A.; Cheeseman, J. R.; Scalmani, G.; Barone, V.; Petersson, G. A.; Nakatsuji, H. et al. Gaussian16 Revision A.03. 2016; Gaussian Inc. Wallingford CT.

(10) Tuladhar, A.; Dewan, S.; Kubicki, J. D.; Borguet, E. Spectroscopy and Ultrafast Vibrational Dynamics of Strongly Hydrogen Bonded OH Species at the -Al2O3(1120)/H2O Interface. *The Journal of Physical Chemistry C* **2016**, *120*, 16153–16161.